

## RADIO EMISSION FROM DIRECT-COLLAPSE BLACK HOLES

DANIEL J. WHALEN<sup>1,2</sup>, MAR MEZCUA<sup>3</sup>, SAMUEL J. PATRICK<sup>1,4</sup>, AVERY MEIKSIN<sup>4</sup> AND MUHAMMAD A. LATIF<sup>5</sup>*Draft version March 17, 2022*

## ABSTRACT

Direct-collapse black holes (DCBHs) forming at  $z \sim 20$  are currently the leading candidates for the seeds of the first quasars, over 200 of which have now been found at  $z > 6$ . Recent studies suggest that DCBHs could be detected in the near infrared by the *James Webb Space Telescope*, *Euclid*, and the *Roman Space Telescope*. However, new radio telescopes with unprecedented sensitivities such as the Square Kilometer Array (SKA) and the Next-Generation Very Large Array (ngVLA) may open another window on the properties of DCBHs in the coming decade. Here we estimate the radio flux from DCBHs at birth at  $z = 8 - 20$  with several fundamental planes of black hole accretion. We find that they could be detected at  $z \sim 8$  by the SKA-FIN all-sky survey. Furthermore, SKA and ngVLA could discover  $10^6 - 10^7 M_\odot$  BHs out to  $z \sim 20$ , probing the formation pathways of the first quasars in the Universe.

*Subject headings:* quasars: supermassive black holes — black hole physics — early universe — dark ages, reionization, first stars — galaxies: formation — galaxies: high-redshift

## 1. INTRODUCTION

Direct-collapse black holes (DCBHs) are one of the leading contenders for the origin of the first quasars in the Universe, over 200 of which have now been found at  $z > 6$  (Mortlock et al. 2011; Bañados et al. 2018; Matsuoka et al. 2019; Wang et al. 2021). They are thought to form when rapidly-accreting supermassive primordial stars in atomically-cooling halos collapse at masses of a few  $10^4 - 10^5 M_\odot$  at  $z \sim 20$  (Hosokawa et al. 2013; Woods et al. 2017, 2021; Herrington et al. 2021). DCBHs may be the seeds of the first supermassive black holes (SMBHs) because it is difficult for ordinary Population III (Pop III) star BHs to grow rapidly after birth (Whalen et al. 2004; Whalen & Fryer 2012; Smith et al. 2018). DCBHs are born with much larger masses and in much higher densities in host halos that can retain their fuel supply, even when it is heated by X-rays (Johnson et al. 2013 – see Woods et al. 2019 for recent reviews).

A number of studies have examined the prospects for detection of supermassive Pop III stars (Surace et al. 2018, 2019) and DCBHs (Pacucci et al. 2015; Natarajan et al. 2017; Barrow et al. 2018; Whalen et al. 2020b) in the near infrared (NIR) by the *James Webb Space Telescope* (*JWST*), *Euclid*, and the *Roman Space Telescope* (*RST*). They found that DCBHs could be detected by *JWST* at  $z \lesssim 20$  and by *Euclid* and *RST* at  $z \lesssim 6 - 8$ , although lensing by galaxy clusters and massive galaxies in their wide fields could extend these detections up to  $z \lesssim 10 - 15$  (Vikaeus et al. 2021). They can be distinguished from primordial galaxies in color-color space in

appropriate NIR filters and from cool, dim foreground stars because they are transients due to fluctuations in accretion flows. DCBHs may also be detected out to  $z \sim 10$  by future X-ray missions such as the *Advanced Telescope for High-Energy Astrophysics* (*ATHENA*) and *Lynx* (Aird et al. 2013).

DCBHs are also expected to be radio sources, and they could be detected by a new generation of observatories with unprecedented sensitivities such as the Square Kilometer Array (SKA) and the next-generation Very Large Array (ngVLA) in the coming decade. Recent estimates of radio power from a DCBH in the Ly $\alpha$  emitter CR7 at  $z = 6.6$  indicate that it could reach  $\sim 100$  nJy at 1.0 GHz, well above the eventual 20 nJy detection limit planned for the SKA-FIN all-sky survey (Whalen et al. 2020a). Nascent DCBHs would be free of competing sources of radio emission in their host halos that are present in CR7, such as young supernova remnants (SNRs; Meiksin & Whalen 2013; Reines et al. 2020) and H II regions due to star formation (Condon 1992), because they form in halos before other stars.

Yue & Ferrara (2021) recently estimated DCBH radio fluxes under the assumption that they drive strong jets and found that they should be detectable by the SKA and ngVLA at  $z \sim 10$ , depending on the inclination angle of the jet. However, steady jets have only been observed in active galactic nuclei with luminosities  $L \lesssim 0.01 L_{\text{Edd}}$ , where  $L_{\text{Edd}}$  is the Eddington limit, and intermittent jets have been seen in quasars at  $L \sim L_{\text{Edd}}$  (Merloni & Heinz 2008). At these accretion rates the disk is geometrically thick and radiatively inefficient. No jets have been found at  $0.01 L_{\text{Edd}} < L < L_{\text{Edd}}$ , when the disk is geometrically thin and radiatively efficient. Recent radiation hydrodynamical simulations of the formation of a  $z = 7.1$  quasar found that the DCBH accretes at 20% - 80% of the Eddington limit at birth, a regime in which no jets are expected to form, but they could not resolve the accretion disk of the BH (Smidt et al. 2018).

We have instead applied fundamental planes of BH accretion to estimate DCBH radio fluxes for a range of redshifts. The accretion rates in these planes are taken from

<sup>1</sup> Institute of Cosmology and Gravitation, Portsmouth University, Dennis Sciamia Building, Portsmouth PO1 3FX

<sup>2</sup> Ida Pfeifer Professor, Department of Astrophysics, University of Vienna, Tuerkenschanzstrasse 17, 1180, Vienna, Austria

<sup>3</sup> Institute of Space Sciences (ICE, CSIC), Campus UAB, Carrer de Magrans, 08193 Barcelona, Spain

<sup>4</sup> Institut d'Estudis Espacials de Catalunya (IEEC), Carrer Gran Capità, 08034 Barcelona, Spain

<sup>5</sup> Institute for Astronomy, University of Edinburgh, Blackford Hill, Edinburgh EH9 3HJ, UK

<sup>6</sup> Physics Department, College of Science, United Arab Emirates University, PO Box 15551, Al-Ain, UAE

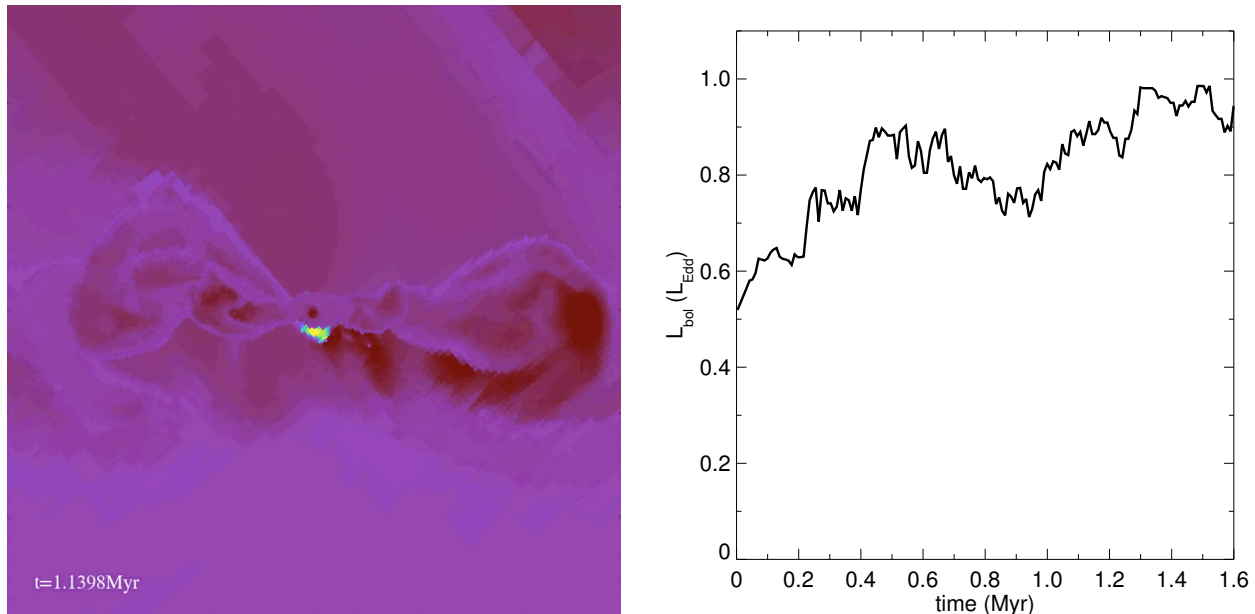


FIG. 1.— Left: temperature image of an atomically-cooled disk surrounding a DCBH 1.14 Myr after birth. An ultracompact H II region (yellow/green) with a radius of  $\sim 0.15$  pc is visible below the midplane of the disk. The X-rays are trapped in the disk because of large ambient densities and the ram pressure of infalling gas. The image is 3 pc on a side. Right: DCBH bolometric luminosity in units of the Eddington rate.

a new cosmological radiation hydrodynamical simulation that resolves flows onto the DCBH on scales of 0.01 pc that have never before been achieved. In Section 2 we discuss our DCBH accretion simulation and radio flux calculations. We calculate radio emission as a function of DCBH mass and redshift and estimate the ngVLA integration times required to detect them in Section 3. We also determine the minimum DCBH masses required for detection by currently planned SKA and ngVLA surveys as a function of redshift and then conclude in Section 4.

## 2. NUMERICAL METHOD

We extract DCBH accretion rates from a cosmological radiation hydrodynamics simulation and use them to estimate DCBH radio fluxes in six fundamental planes of BH accretion. We also estimate the flux from the ultracompact H II region formed by X-rays from the BH to determine if it is an important source of radio emission.

### 2.1. DCBH Bolometric Luminosities

Our DCBH simulation is performed with the Enzo adaptive mesh refinement (AMR) cosmology code (Bryan et al. 2014). Our simulation box is  $1.5 h^{-1}$  Mpc with a  $256^3$  root grid and three nested grids centered on the halo for an effective initial resolution of  $2048^3$ . We initialize the run at  $z = 200$  with Gaussian random perturbations calculated with MUSIC (Hahn & Abel 2011) and allow up to 15 levels of AMR after the onset of atomic cooling in the halo for a maximum resolution of 0.014 pc. We use second-year *Planck* cosmological parameters:  $\Omega_M = 0.308$ ,  $\Omega_\Lambda = 0.691$ ,  $\Omega_b h^2 = 0.0223$ ,  $\sigma_8 = 0.816$ ,  $h = 0.677$  and  $n = 0.968$  (Planck Collaboration et al. 2016).

We include six-species nonequilibrium primordial gas chemistry (H, He,  $e^-$ ,  $H^+$ ,  $He^+$ ,  $H^{2+}$ ) without  $H_2$  to ensure isothermal cooling and collapse. X-rays from the

DCBH are propagated in the box with the MORAY radiation transport package (Wise & Abel 2011). Ionizations and Compton heating due to X-rays and secondary ionizations by energetic photoelectrons are included in the chemistry and gas energy equations along with the usual primordial cooling processes: collisional excitational and ionizational cooling by H and He, recombinational cooling, bremsstrahlung cooling, and inverse Compton cooling by the cosmic microwave background (CMB).

The halo in our model begins to atomically cool when it reaches a mass of  $1.44 \times 10^7 M_\odot$  at  $z = 17$  and forms a massive disk at its center. At this point we turn on 1 keV X-rays from a  $10^5 M_\odot$  DCBH at the center of the disk and evolve it for 1.66 Myr. We show an edge-on view of the disk in the left panel of Figure 1 at 1.14 Myr. It is approximately 3 pc in diameter, and the nascent ultracompact (UC) H II region of the BH is visible at its center with a radius of  $\sim 0.15$  pc and temperature of  $\sim 5 \times 10^6$  K. Radiation from the BH remains trapped deep in the disk throughout the run because of gas densities that exceed  $10^{10} \text{ cm}^{-3}$  and large ram pressures due to heavy infall that can reach  $1 M_\odot \text{ yr}^{-1}$ . We plot the bolometric luminosity,  $L_{\text{bol}}$ , for the DCBH in the right panel of Figure 1. There are fluctuations due to turbulent flows in the disk but they average  $\sim 0.85 L_{\text{Edd}}$ . This luminosity is consistent with those at early times in Smidt et al. (2018) so we use it in our study.

### 2.2. Fundamental Plane Radio Fluxes

Fundamental planes of black hole accretion (FPs) are correlations between the mass of a BH,  $M_{\text{BH}}$ , its nuclear X-ray luminosity at 2 - 10 keV,  $L_X$ , and its nuclear radio luminosity at 5 GHz,  $L_R$  (Merloni et al. 2003; see Mezcua et al. 2018 for a brief review). FPs extend over six orders of magnitude in BH mass, including down to the intermediate mass black hole (IMBH) regime ( $< 10^5$

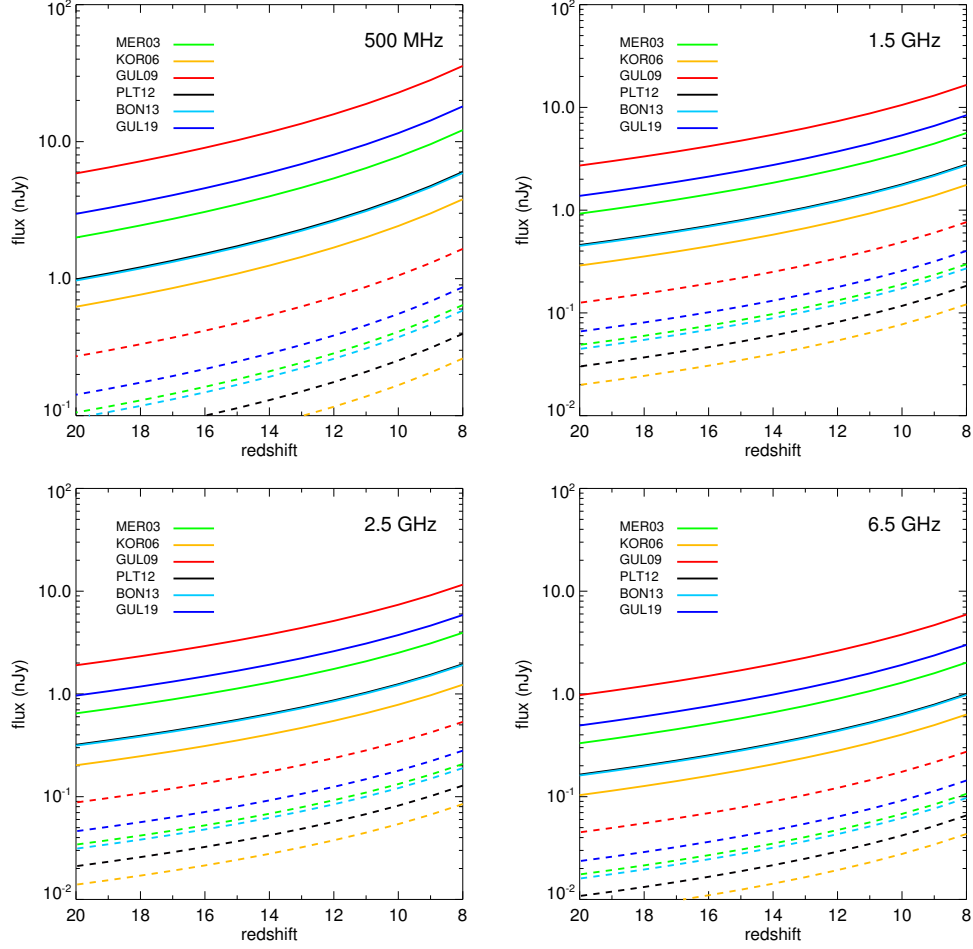


FIG. 2.— Radio fluxes for  $10^5 M_\odot$  (dashed) and  $10^6 M_\odot$  (solid) DCBHs at  $z = 8 - 20$  from 6 FPs. Upper left: 500 MHz. Upper right: 1.5 GHz. Lower left: 2.5 GHz. Lower right: 6.5 GHz.

$M_\odot$ ; Gültekin et al. 2014). To estimate the flux from a DCBH in a given radio band in the observer frame we first use an FP to calculate  $L_R$  in the rest frame, which depends on  $M_{\text{BH}}$  and  $L_X$ . We calculate  $L_X$  from  $L_{\text{bol}}$  with Equation 21 of Marconi et al. (2004),

$$\log \left( \frac{L_{\text{bol}}}{L_X} \right) = 1.54 + 0.24\mathcal{L} + 0.012\mathcal{L}^2 - 0.0015\mathcal{L}^3, \quad (1)$$

where  $\mathcal{L} = \log L_{\text{bol}} - 12$  and  $L_{\text{bol}}$  is in units of solar luminosity.  $L_R$  can then be obtained from  $L_X$  with an FP of the form

$$\log L_R = \alpha \log L_X + \beta \log M_{\text{BH}} + \gamma, \quad (2)$$

where  $\alpha$ ,  $\beta$  and  $\gamma$  for FPs from Merloni et al. (2003, MER03), Körding et al. (2006, KOR06), Gültekin et al. (2009, GUL09), Plotkin et al. (2012, PLT12), and Bonchi et al. (2013, BON13) are listed in Table 1 of Whalen et al. (2020a). We also consider the FP of Equation 19 in Gültekin et al. (2019, GUL19),

$$R = -0.62 + 0.70 X + 0.74 \mu, \quad (3)$$

where  $R = \log(L_R/10^{38}\text{erg/s})$ ,  $X = \log(L_X/10^{40}\text{erg/s})$  and  $\mu = \log(M_{\text{BH}}/10^8 M_\odot)$ .

Since radio flux from a DCBH that is cosmologically redshifted into a given observer band does not originate from 5 GHz in the source frame, we calculate it from  $L_R = \nu L_\nu$ , assuming that the spectral luminosity  $L_\nu \propto \nu^{-\alpha}$  with a spectral index  $\alpha = 0.7$  (Condon et al. 2002). The spectral flux at  $\nu$  in the observer frame is then determined from the spectral luminosity at  $\nu'$  in the rest frame with

$$F_\nu = \frac{L_{\nu'}(1+z)}{4\pi d_L^2}, \quad (4)$$

where  $d_L$  is the luminosity distance and  $\nu' = (1+z)\nu$ . We plot radio fluxes for  $10^5$  and  $10^6 M_\odot$  DCBHs at 0.85  $L_{\text{Edd}}$  at 500 MHz, 1.5 GHz, 2.5 GHz and 6.5 GHz for all six FPs at  $z = 8 - 20$  in Figure 2.

### 2.3. UC H II Region Flux

The UC H II region of the DCBH in principle can also be a source of synchrotron and bremsstrahlung radio emission that is not included in the FPs, which only consider emission due to the inner accretion disk of the BH and its interaction with its immediate environment. At a density of  $\sim 10^4 \text{ cm}^{-3}$ , temperature of  $\sim 5 \times 10^6 \text{ K}$  and a maximum radius of 0.5 pc (this radius fluctuates with flows onto the DCBH), the UC H II region will

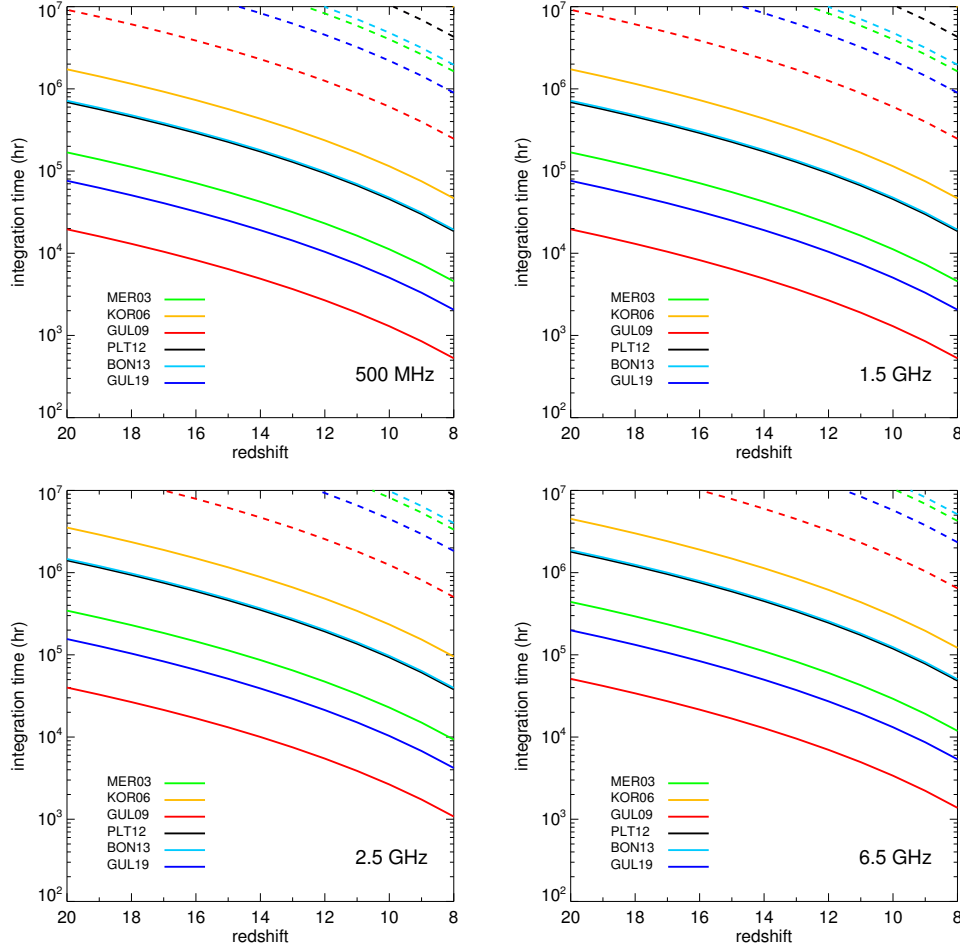


FIG. 3.— Integration times required to detect radio emission from  $10^5 M_\odot$  (dashed) and  $10^6 M_\odot$  (solid) DCBHs at  $z = 8 - 20$ . Upper left: 500 MHz SKA band. Upper right: 1.5 GHz ngVLA band. Lower left: 2.5 GHz ngVLA band. Lower right: 6.5 GHz ngVLA band.

be optically thick to free-free emission at rest frequencies below 71 MHz. Consequently, it will shine like a black body at  $T = 5 \times 10^6$  K at these frequencies. For emission at frequency  $\nu'$  by an H II region of radius  $R$  at redshift  $z$ , the received flux at frequency  $\nu = \nu'/(1+z)$  is

$$F_\nu = \frac{2\pi kT}{\lambda'^2} (1+z) \frac{R}{d_L^2}, \quad (5)$$

where  $\lambda' = c/\nu'$ . For  $z = 9$  and our cosmological parameters, this becomes

$$F_\nu = 1.4 \times 10^{-5} \text{ nJy} \left( \frac{\nu'}{1 \text{ MHz}} \right)^2. \quad (6)$$

Besides lying well below SKA and ngVLA bands, these fluxes would be far too low to be observed, and they represent an upper limit because the UC H II region would be optically thin to radio frequencies above 71 MHz and would thus likely be dimmer at the frequencies considered in this paper.

### 3. DCBH RADIO POWER

The SKA-FIN all-sky survey will reach 20 nJy at all 4 frequencies considered here and the ngVLA can reach 45 nJy at 3.5 - 12.3 GHz and 78 nJy at 1.2 - 3.5 GHz with

24 hr integration times (Plotkin & Reines 2018). Our calculations show that  $10^6 M_\odot$  DCBHs could be found by the SKA-FIN survey at 500 MHz out to  $z = 11$  but detections by the ngVLA at 1.5 - 6.5 MHz will require integration times greater than 24 hr.

We plot these integration times for  $z = 8 - 20$  in Figure 3. With total exposures of 1000 - 2000 hr, ngVLA could detect  $10^6 M_\odot$  DCBHs at  $z = 8 - 10$ . This is the redshift range over which some models predict that the comoving number density of DCBHs is highest (see, e.g., Figure 4 of Valiante et al. 2017) so both observatories can detect these objects at the times at which their numbers are greatest. However, we find that DCBHs with masses  $\lesssim 10^5 M_\odot$  will remain beyond the reach of these telescopes for now.

In Figure 4 we show the minimum DCBH mass required for detection by the SKA-FIN survey and by the ngVLA with a 24-hr integration time. The least massive one that could be detected by currently proposed surveys would be a  $6.5 \times 10^5 M_\odot$  DCBH at  $z = 8$  at 500 MHz by SKA-FIN. However, this survey could find BHs ranging in mass from  $2.5 \times 10^6 M_\odot$  to  $2.2 \times 10^7 M_\odot$  at  $z = 20$  and ngVLA could detect  $10^7 - 10^8 M_\odot$  BHs at  $z = 15 - 20$ . Such detections at high redshifts could probe the origins of the first quasars and distinguish between

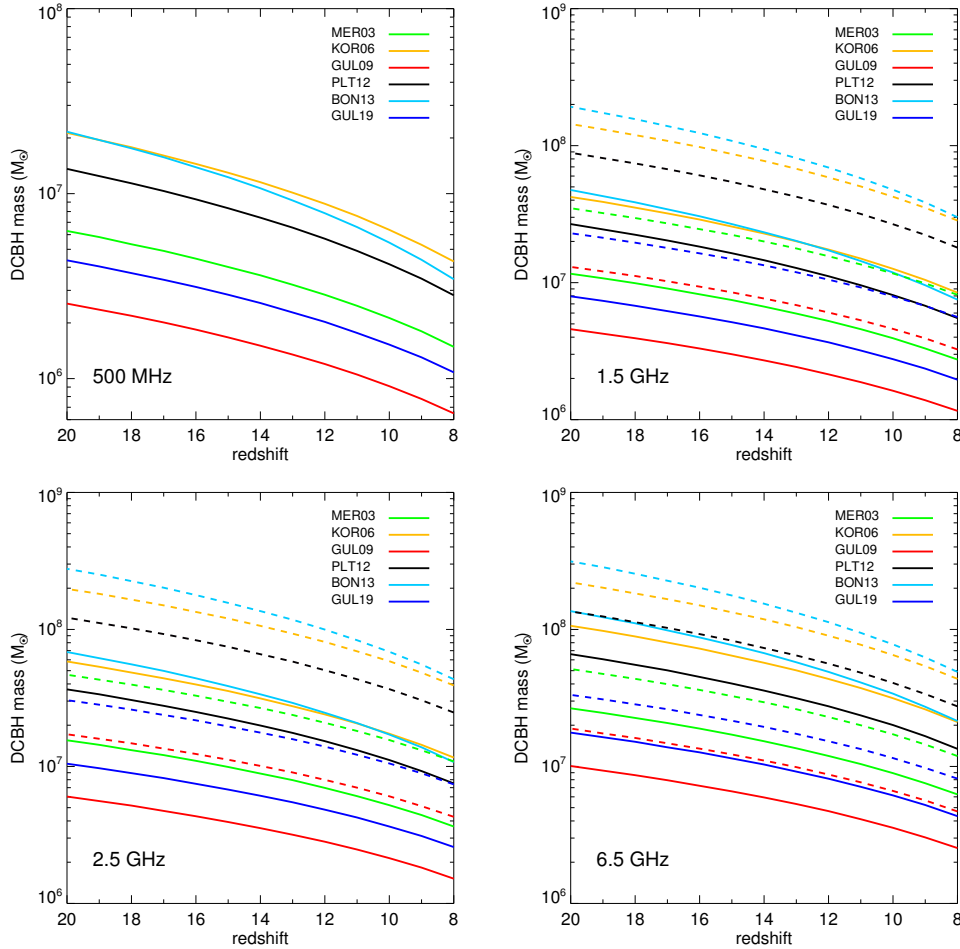


FIG. 4.— Threshold DCBH masses that could be detected in the SKA-FIN survey (solid) and a 24-hr integration time ngVLA survey (dashed) at  $z = 8 - 20$ . Upper left: 500 MHz SKA band. Upper right: 1.5 GHz ngVLA and SKA bands. Lower left: 2.5 GHz ngVLA and SKA bands. Lower right: 6.5 GHz ngVLA and SKA bands.

channels for their formation, such as Pop III stars or very massive stars formed in intermediate Lyman-Werner UV backgrounds (Patrick et al. 2021).

#### 4. DISCUSSION AND CONCLUSION

The SKA could detect DCBHs at birth at  $z = 8 - 9$ , when their comoving number densities may be highest, but only more massive, evolved BHs could be detected at higher redshifts (Whalen & Mezcua 2021). Radio flux from these BHs may be contaminated by emission from H II regions and SNRs in their host galaxies, which would host active star formation (Smidt et al. 2018). However, Whalen et al. (2020a) found that in CR7, the brightest Ly $\alpha$  emitter at  $z > 6$  and which hosts rapid star formation, these competing sources of radio flux were either too small to be detected or could be distinguished from flux from a  $4 \times 10^6 M_\odot$  DCBH. Mezcua et al. (2019) detected IMBHs in dwarf galaxies by subtracting contributions to their radio signals from these additional sources. Here, we only consider the most massive DCBHs forming in purely atomically-cooling halos (e.g., Patrick et al. 2020), but less massive objects forming in lower LW backgrounds ( $10^3 M_\odot - 10^4 M_\odot$ ) may have been more common in the primordial universe (Latif et al. 2020). Our

calculations show that these IMBHs would not be visible at birth and would have to grow in mass by at least a factor of ten to be found at later epochs.

Our radio fluxes ignore contributions from DCBH jets but they are not thought to be important for two reasons. First, as discussed earlier, jets are not expected at the accretion rates we found for DCBHs at birth. Second, even if a DCBH launches a jet, its radio emission may be quenched by the CMB at high redshifts. If the energy density of CMB photons (which rises as  $z^4$ ) exceeds the magnetic field energy density in the lobes of the jet, relativistic electrons preferentially cool by upscattering CMB photons instead of synchrotron radiation. The absence of radio emission from some high-redshift quasars has been attributed to this process (e.g., Fabian et al. 2014).

The SKA and ngVLA could, in synergy with *JWST*, *Euclid*, and the *RST*, probe the origins and numbers of the first quasars because they could detect BHs that are a few  $10^6 - 10^7 M_\odot$  out to  $z = 20$  in the coming decade. Redshift cutoffs above which such objects are not observed in the radio could distinguish between seeding mechanisms for the first SMBHs, whether they come from ordinary Pop III stars, supermassive primor-

dial stars, or are the result of runaway stellar collisions in dense nuclear clusters at high redshifts. However, modeling the radio emission from this primordial population of low-mass quasars would require cosmological simulations of star formation rates in their host galaxies to discriminate between competing sources of radio emission in them, such as SNRs and H II regions. These models are now under development.

D.J.W. was supported by the Ida Pfeiffer Professorship at the Institute of Astrophysics at the University

of Vienna. MM acknowledges support from the Beatriu de Pinos fellowship (2017-BP-00114) and from the Ramon y Cajal fellowship (RYC2019-027670-I). S.P. was supported by STFC grant ST/N504245/1. A. M. acknowledges support from the UK Science and Technology Facilities Council Consolidated Grant ST/R000972/1. M.L. acknowledges funding from UAEU via UPAR grant No. 31S372. Our calculations were performed on the Sciama HPC cluster at the Institute of Cosmology and Gravitation at the University of Portsmouth.

## REFERENCES

- Aird, J., et al. 2013, arXiv e-prints, arXiv:1306.2325
- Bañados, E., et al. 2018, *Nature*, 553, 473
- Barrow, K. S. S., Aykutalp, A., & Wise, J. H. 2018, *Nature Astronomy*, 2, 987
- Bonchi, A., La Franca, F., Melini, G., Bongiorno, A., & Fiore, F. 2013, *MNRAS*, 429, 1970
- Bryan, G. L., et al. 2014, *ApJS*, 211, 19
- Condon, J. J. 1992, *ARA&A*, 30, 575
- Condon, J. J., Cotton, W. D., & Broderick, J. J. 2002, *AJ*, 124, 675
- Fabian, A. C., Walker, S. A., Celotti, A., Ghisellini, G., Mocz, P., Blundell, K. M., & McMahon, R. G. 2014, *MNRAS*, 442, L81
- Gültekin, K., Cackett, E. M., King, A. L., Miller, J. M., & Pinkney, J. 2014, *ApJ*, 788, L22
- Gültekin, K., Cackett, E. M., Miller, J. M., Di Matteo, T., Markoff, S., & Richstone, D. O. 2009, *ApJ*, 706, 404
- Gültekin, K., King, A. L., Cackett, E. M., Nyland, K., Miller, J. M., Di Matteo, T., Markoff, S., & Rupen, M. P. 2019, *ApJ*, 871, 80
- Hahn, O., & Abel, T. 2011, *MNRAS*, 415, 2101
- Herrington, N., Whalen, D. J., & Wood, T. E. 2021, *MNRAS*, in prep
- Hosokawa, T., Yorke, H. W., Inayoshi, K., Omukai, K., & Yoshida, N. 2013, *ApJ*, 778, 178
- Johnson, J. L., Whalen, D. J., Li, H., & Holz, D. E. 2013, *ApJ*, 771, 116
- Körding, E., Falcke, H., & Corbel, S. 2006, *A&A*, 456, 439
- Latif, M. A., Khochfar, S., Schleicher, D., & Whalen, D. J. 2020, arXiv e-prints, arXiv:2012.09177
- Marconi, A., Risaliti, G., Gilli, R., Hunt, L. K., Maiolino, R., & Salvati, M. 2004, *MNRAS*, 351, 169
- Matsuoka, Y., et al. 2019, *ApJ*, 872, L2
- Meiksin, A., & Whalen, D. J. 2013, *MNRAS*, 430, 2854
- Merloni, A., & Heinz, S. 2008, *MNRAS*, 388, 1011
- Merloni, A., Heinz, S., & di Matteo, T. 2003, *MNRAS*, 345, 1057
- Mezcua, M., Hlavacek-Larrondo, J., Lucey, J. R., Hogan, M. T., Edge, A. C., & McNamara, B. R. 2018, *MNRAS*, 474, 1342
- Mezcua, M., Suh, H., & Civano, F. 2019, *MNRAS*, 488, 685
- Mortlock, D. J., et al. 2011, *Nature*, 474, 616
- Natarajan, P., Pacucci, F., Ferrara, A., Agarwal, B., Ricarte, A., Zackrisson, E., & Cappelluti, N. 2017, *ApJ*, 838, 117
- Pacucci, F., Ferrara, A., Volonteri, M., & Dubus, G. 2015, *MNRAS*, 454, 3771
- Patrick, S., Whalen, D. J., Elford, J. S., & Latif, M. 2021, *MNRAS*, in prep
- Patrick, S. J., Whalen, D. J., Elford, J. S., & Latif, M. A. 2020, arXiv e-prints, arXiv:2012.11612
- Planck Collaboration et al. 2016, *A&A*, 594, A13
- Plotkin, R. M., Markoff, S., Kelly, B. C., Körding, E., & Anderson, S. F. 2012, *MNRAS*, 419, 267
- Plotkin, R. M., & Reines, A. E. 2018, arXiv:1810.06814, arXiv:1810.06814
- Reines, A. E., Condon, J. J., Darling, J., & Greene, J. E. 2020, *ApJ*, 888, 36
- Smidt, J., Whalen, D. J., Johnson, J. L., Surace, M., & Li, H. 2018, *ApJ*, 865, 126
- Smith, B. D., Regan, J. A., Downes, T. P., Norman, M. L., O’Shea, B. W., & Wise, J. H. 2018, *MNRAS*, 480, 3762
- Surace, M., Zackrisson, E., Whalen, D. J., Hartwig, T., Glover, S. C. O., Woods, T. E., Heger, A., & Glover, S. C. O. 2019, *MNRAS*, 488, 3995
- Surace, M., et al. 2018, *ApJ*, 869, L39
- Valiante, R., Agarwal, B., Habouzit, M., & Pezzulli, E. 2017, *PASA*, 34, e031
- Vikaeus, A. F., Zackrisson, E., & Whalen, D. J. 2021, *ApJ*, in prep
- Wang, F., et al. 2021, *ApJ*, 907, L1
- Whalen, D., Abel, T., & Norman, M. L. 2004, *ApJ*, 610, 14
- Whalen, D. J., & Fryer, C. L. 2012, *ApJ*, 756, L19
- Whalen, D. J., & Mezcua, M. 2021, *MNRAS*, in prep
- Whalen, D. J., Mezcua, M., Meiksin, A., Hartwig, T., & Latif, M. A. 2020a, *ApJ*, 896, L45
- Whalen, D. J., Surace, M., Bernhardt, C., Zackrisson, E., Pacucci, F., Ziegler, B., & Hirschmann, M. 2020b, *ApJ*, 897, L16
- Wise, J. H., & Abel, T. 2011, *MNRAS*, 414, 3458
- Woods, T. E., Heger, A., Whalen, D. J., Haemmerlé, L., & Klessen, R. S. 2017, *ApJ*, 842, L6
- Woods, T. E., Patrick, S., Elford, J. S., Whalen, D. J., & Heger, A. 2021, *ApJ*, 915, 110
- Woods, T. E., et al. 2019, *Publications of the Astronomical Society of Australia*, 36, e027
- Yue, B., & Ferrara, A. 2021, arXiv e-prints, arXiv:2107.11307